
Partition-wise Linear Models

Hidekazu Oiwa*

Graduate School of Information Science and Technology
The University of Tokyo
hidekazu.oiwa@gmail.com

Ryohei Fujimaki

NEC Laboratories America
rfujimaki@nec-labs.com

Abstract

Region-specific linear models are widely used in practical applications because of their non-linear but highly interpretable model representations. One of the key challenges in their use is non-convexity in simultaneous optimization of regions and region-specific models. This paper proposes novel convex region-specific linear models, which we refer to as partition-wise linear models. Our key ideas are 1) assigning linear models not to regions but to partitions (region-specifiers) and representing region-specific linear models by linear combinations of partition-specific models, and 2) optimizing regions via partition selection from a large number of given partition candidates by means of convex structured regularizations. In addition to providing initialization-free globally-optimal solutions, our convex formulation makes it possible to derive a generalization bound and to use such advanced optimization techniques as proximal methods and decomposition of the proximal maps for sparsity-inducing regularizations. Experimental results demonstrate that our partition-wise linear models perform better than or are at least competitive with state-of-the-art region-specific or locally linear models.

1 Introduction

Among pre-processing methods, data partitioning is one of the most fundamental. In it, an input space is divided into several sub-spaces (regions) and assigned a simple model for each region. In addition to better predictive performance resulting from the non-linear nature that arises from multiple partitions, the regional structure also provides a better understanding of data (i.e., better interpretability). Region-specific linear models learn both partitioning structures and predictors in each region.

Such models vary—from traditional decision/regression trees [1] to more advanced models [2, 3, 4]—depending on their region-specifiers (how they characterize regions), region-specific prediction models, and the objective functions to be optimized. One important challenge that remains in learning these models is the non-convexity that arises from the inter-dependency of optimizing regions and prediction models in individual regions. Most previous work suffers from disadvantages arising from non-convexity, including initialization-dependency (bad local minima) and lack of generalization error analysis.

This paper proposes convex region-specific linear models. We refer to them as partition-wise linear models. Our models have two distinguishing characteristics that help avoid the non-convexity problem.

*The work reported here was conducted when the first author was a visiting researcher at NEC Laboratories America.

Table 1: Comparison of region-specific and locally linear models.

	Ours	LSL-SP	CSTC	LDKL	FaLK-SVMs	LLSVMs
Region Optimization	✓	✓	✓	✓		
Initialization-independent	✓					✓
Generalization Bound	✓	✓			✓	
Region Specifiers	(Sec. 2.2)	Linear	Linear	Linear	Non-Regional	Non-Regional

Partition-wise Modeling We propose partition-wise linear models as a novel class of region-specific linear models. Our models divide an input space by means of a small set of partitions¹. Each partition possesses one weight vector, and this weight vector is only applied to one side of the divided space. It is trained to represent the local relationship between input vectors and output values. Region-specific predictors are constructed by linear combinations of these weight vectors. Our partition-wise parameterization enables us to construct convex objective functions.

Convex Optimization via Sparse Partition Selection We optimize regions by selecting effective partitions from a large number of given candidates, using convex sparsity-inducing structured regularizations. In other words, we trade continuous region optimization for convexity. We allow partitions to locate only given discrete candidate positions, and are able to derive convex optimization problems. We have developed an efficient algorithm to solve structured-sparse optimization problems, and in it we utilize both a proximal method [5, 6] and the decomposition of proximal maps [7].

As a reliable partition-wise linear model, we have developed a global and local residual model that combines one global model and a set of partition-wise linear models. Further, our theoretical analysis gives a generalization bound for this model. Its large number of partition candidates enables us to obtain relatively low empirical error, but it leads to an increase in the risk of over-fitting. Our generalization bound analysis indicates that we can increase the number of partition candidates by less than an exponential order with respect to the number of samples, which is large enough to achieve good predictive performance in practice. Experimental results have demonstrated that our proposed models perform better than or are at least competitive with state-of-the-art region-specific or locally linear models.

1.1 Related Work

Region-specific linear models and locally linear models are the most closely related models to our own. The former category, to which our models belong, assumes one predictor in a specific region and has an advantage in clear model interpretability, while the latter assigns one predictor to every single datum and has an advantage in higher model flexibility. Interpretable models are able to indicate clearly where and how the relationships between inputs and outputs change.

Well-known precursors to region-specific linear models are decision/regression trees [1], which use rule-based region-specifiers and constant-valued predictors. Another traditional framework is a hierarchical mixture of experts [8], which is a probabilistic tree-based region-specific model framework. Recently, Local Supervised Learning through Space Partitioning (LSL-SP) has been proposed [3]. LSL-SP utilizes a linear-chain of linear region-specifiers as well as region-specific linear predictors. The highly important advantage of LSL-SP is the upper bound of generalization error analysis via the VC dimension. Additionally, a Cost-Sensitive Tree of Classifiers (CSTC) algorithm has also been developed [4]. It utilizes a tree-based linear localizer and linear predictors. This algorithm’s uniqueness among other region-specific linear models is in its taking “feature utilization cost” into account for test time speed-up. Although the developers’ formulation with sparsity-inducing structured regularization is, in a way, related to ours, their model representations and, more importantly, their motivation (test time speed-up) is different from ours.

¹In our paper, a region is a sub-space in an input space. Multiple regions do not intersect each other, and, in their entirety, they cover the whole input space. A partition is an indicator function that divides an input space into two parts.

Table 2: Basic Notations

N, n	# of data and index
D, d	# of dimensions and index
P, p	# of partitions and index
x_n, y_n	n -th input and output
a_p	p -th weight vector
A	weight matrix
$f_p(\cdot)$	p -th activeness function
$f(\cdot)$	activeness vector
$g(\cdot)$	partition-wise linear predictor
$\ell(\cdot, \cdot)$	loss function

Fast Local Kernel Support Vector Machines (FaLK-SVMs) represent state-of-the-art locally linear models. FaLK-SVMs produce test-point-specific weight vectors by learning local predictive models from the neighborhoods of individual test points [9]. It aims to reduce prediction time cost by pre-processing for nearest-neighbor calculations and local model sharing, at the cost of initialization-independency. Another advanced locally linear model is that of Locally Linear Support Vector Machines (LLSVMs) [10]. LLSVMs assign linear SVMs to multiple anchor points produced by manifold learning [11, 12] and construct test-point-specific linear predictors according to the weights of anchor points with respect to individual test points. When the manifold learning procedure is initialization-independent, LLSVMs become initial-value-independent because of the convexity of the optimization problem. Similarly, clustered SVMs (CSVMs) [13] assume given data clusters and learn multiple SVMs for individual clusters simultaneously. Although CSVMs are convex and generalization bound analysis has been provided, they cannot optimize regions (clusters).

Joes et al. have proposed Local Deep Kernel Learning (LDKL) [2], which adopts an intermediate approach with respect to region-specific and locally linear models. LDKL is a tree-based local kernel classifier in which the kernel defines regions and can be seen as performing region-specification. One main difference from common region-specific linear models is that LDKL changes kernel combination weights for individual test points, and therefore the predictors are locally determined in every single region. Its aim is to speed up kernel SVMs’ prediction while maintaining the non-linear ability.

Table 1 summarizes the above described state-of-the-art models in contrast with ours from a number of significant perspectives. Our proposed model uniquely exhibits three properties: joint optimization of regions and region-specific predictors, initialization-independent optimization, and meaningful generalization bound.

1.2 Notations

Scalars and vectors are denoted by lower-case x . Matrices are denoted by upper-case X . Training samples and labels are denoted by $x_n \in \mathbb{R}^D$ and y_n . The basic notations used in this paper are summarized in Table 2.

2 Partition-wise Linear Models

This section explains partition-wise linear models under the assumption that effective partitioning is already known and fixed. We discuss how to optimize partitions and region-specific linear models in Section 3.

2.1 Framework

Figure 1 illustrates the concept of partition-wise linear models. Suppose we have P partitions (red dashed lines) which essentially specify 2^P regions. Partition-wise linear models are defined as follows. First, we assign a linear weight vector a_p to the p -th partition. This partition has an *activeness function*, f_p , which indicates whether the attached weight vector a_p is applied to individual data

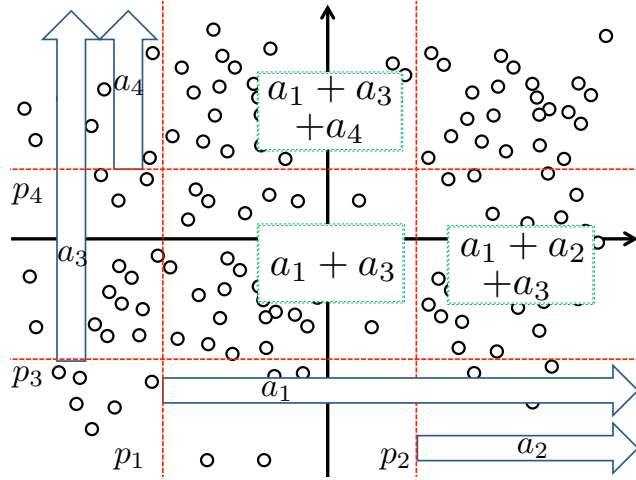


Figure 1: Concept of Partition-wise Linear Models

points or not. For example, in Figure 1, we set the weight vector a_1 to be applied to the right-hand side of partition p_1 . In this case, the corresponding activeness function is defined as $f_1(x) = 1$ when x is in the right-hand side of p_1 . Second, region-specific predictors (squared regions surrounded by partitions in Figure 1) are defined by a linear combination of active partition-wise weight vectors that are also linear models.

Let us formally define the partition-wise linear models. We have a set of given activeness functions, f_1, \dots, f_P , which is denoted in a vector form as $f(\cdot) = (f_1(\cdot), \dots, f_P(\cdot))^T$. The p -th element $f_p(x) \in \{0, 1\}$ indicates whether the attached weight vector a_p is applied to x or not. The activeness function $f(\cdot)$ can represent at most 2^P regions, and $f(x)$ specifies to which region x belongs. A linear model of an individual region is then represented as $\sum_{p=1}^P f_p(\cdot) a_p$. It is worth noting that partition-wise linear models use P linear weight vectors to represent 2^P regions and restrict the number of parameters.

The overall predictor $g(\cdot)$ can be denoted as follows:

$$g(x) = \sum_p f_p(x) \sum_d a_{dp} x_d. \quad (1)$$

Let us define A as $A = (a_1, \dots, a_P)$. The partition-wise linear model (1) simply acts as a linear model w.r.t. A while it captures the non-linear nature of data (individual regions use different linear models). Such non-linearity originates from the activeness functions f_p s, which are fundamentally important components in our models.

By introducing a convex loss function $\ell(\cdot, \cdot)$ (e.g., squared loss for regression, squared hinge or logistic loss for classification), we can represent an objective function of the partition-wise linear models as a convex loss minimization problem as follows:

$$\min_A \sum_n \ell(y_n, \sum_p f_p(x_n) \sum_d a_{dp} x_{nd}). \quad (2)$$

Here we give a convex formulation of region-specific linear models under the assumption that a set of partitions is given. In Section 3, we propose a convex optimization algorithm for partitions and regions as a partition selection problem, using sparsity-inducing structured regularization.

2.2 Partition Activeness Functions

A partition activeness function f_p divides the input space into two regions, and a set of activeness functions defines the entire region-structure. Although any function is applicable in principle to being used as a partition activeness function, we prefer as simple a region representation as possible

because of our practical motivation of utilizing region-specific linear models (i.e., interpretability is a priority). This paper restricts them to being parallel to the coordinates, e.g., $f_p(x) = 1$ ($x_i > 2.5$) and $f_p(x) = 0$ (otherwise) with respect to the i -th coordinate. Although this “rule-representation” is simpler than others [2, 3] which use dense linear hyperplanes as region-specifiers, our empirical evaluation (Section 5) indicates that our partition-wise linear models perform competitively with or even better than those others by appropriately optimizing the simple region-specifiers (partition activeness functions).

2.3 Global and Local Residual Model

As a special instance of partition-wise linear models, we here propose a model which we refer to as a global and local residual model. It employs a global linear weight vector a_0 in addition to partition-wise linear weights. The global weight vector is active for all data. The predictor model (1) can be rewritten as:

$$g(x) = a_0^T x + \sum_p f_p(x) \sum_d a_{dp} x_d . \quad (3)$$

The integration of the global weight vector enables the model to determine how features affect outputs not only locally but also globally. Let us consider a new partition activeness function $f_0(x)$ that always returns to 1 regardless of x . Then, by setting $f(\cdot) = (f_0(\cdot), f_1(\cdot), \dots, f_p(\cdot), \dots, f_P(\cdot))^T$ and $A = (a_0, a_1, \dots, a_P)$, the global and local residual model can be represented using the same notation as is used in Section 2.1. Although a_0 and a_p have no fundamental difference here, they are different in terms of how we regularize them (Section 3.1).

3 Convex Optimization of Regions and Predictors

In Section 2, we presented a convex formulation of partition-wise linear models in (2) under the assumption that a set of partition activeness functions was given. This section relaxes this assumption and proposes a convex partition optimization algorithm.

3.1 Region Optimization as Sparse Partition Selection

Let us assume that we have been given $P + 1$ partition activeness functions, f_0, f_1, \dots, f_P , and their attached linear weight vectors, a_0, a_1, \dots, a_P , where f_0 and a_0 are the global activeness function and weight vector, respectively. We formulate the region optimization problem here as partition selection by setting most of a_p s to zero since $a_p = 0$ corresponds to the situation in which the p -th partition does not exist.

Formally, we formulate our optimization problem with respect to regions and weight vectors by introducing two types of sparsity-inducing constraints to (2) as follows:

$$\min_A \sum_n \ell(y_n, g(x_n)) \quad \text{s.t.} \quad \sum_{p \in \{1, \dots, P\}} 1_{\{a_p \neq 0\}} \leq \mu_P, \quad \|a_p\|_0 \leq \mu_0 \quad \forall p. \quad (4)$$

The former constraint restricts the number of effective partitions to at most μ_P . Note that we do not enforce this sparse partition constraint to the global model a_0 so as to be able to determine local trends as residuals from a global trend. The latter constraint restricts the number of effective features of a_p to at most μ_0 . We add this constraint because 1) it is natural to assume only a small number of features are locally effective in practical applications and 2) a sparser model is typically preferred for our purposes because of its better interpretability.

3.2 Convex Optimization via Decomposition of Proximal Maps

3.2.1 The Tightest Convex Envelope

The constraints in (5) are non-convex, and it is very hard to find the global optimum due to the indicator functions and L_0 penalties. This makes optimization over a non-convex region a very complicated task, and we therefore apply a convex relaxation. One standard approach to convex

relaxation would be a combination of group L_1 (the first constraint) and L_1 (the second constraint) penalties. Here, however, we consider the tightest convex relaxation of (4) as follows:

$$\min_A \sum_n \ell(y_n, g(x_n)) \text{ s.t. } \sum_{p=1}^P \|a_p\|_\infty \leq \mu_P, \sum_{d=1}^D \|a_{dp}\|_\infty \leq \mu_0 \quad \forall p. \quad (5)$$

The tightness of constraints in (5) can be shown as follows. The original constraints are non-convex cardinality functions on A , which can be equivalently rewritten in terms of a non-decreasing sub-modular function F on an index set S as:

$$\sum_{\{G_p: S \cap G_p \neq \emptyset\}} 1 \leq \eta_P, \quad \sum_{\{G_{dp}: S \cap G_{dp} \neq \emptyset\}} 1 \leq \eta_0, \quad (6)$$

S is a set of index pairs with respect to non-zero elements in A . G_p is a set of index pairs which correspond to individual features in the p -th partition, i.e., $G_p = \{(d, p) : d \in \{1, \dots, D\}\}$. G_{dp} is a set of single index pairs, i.e., $G_{dp} = \{(d, p)\}$. It is easy to confirm that the constraints in (5) represent the Lovász extension of the constraints in (4), and this extension gives the tightest convex envelope of non-decreasing sub-modular functions [14].

Through such a convex envelope of constraints, the feasible region becomes convex. Therefore, we can reformulate (5) to the following equivalent problem:

$$\min_A \sum_n \ell(y_n, g(x_n)) + \Omega(A) \text{ where } \Omega(A) = \lambda_P \sum_{p=1}^P \|a_p\|_\infty + \lambda_0 \sum_{p=0}^P \sum_{d=1}^D \|a_{dp}\|_\infty. \quad (7)$$

where λ_P and λ_0 are regularization weights corresponding to μ_P and μ_0 , respectively.

This paper derives an efficient optimization algorithm for (7) using the proximal method and the decomposition of proximal maps.

3.2.2 Proximal Method and FISTA

The proximal method is a standard efficient tool for solving convex optimization problems with non-differential regularizers. It iteratively applies gradient steps and proximal steps to update parameters. This achieves $O(1/t)$ convergence [5] under Lipschitz-continuity of the loss gradient, or even $O(1/t^2)$ convergence if an acceleration technique, such as a fast iterative shrinkage thresholding algorithm (FISTA) [6, 15], is incorporated.

Let us define $A^{(t)}$ as the weight matrix at the t -th iteration. In the gradient step, the weight vectors are updated to decrease empirical loss through the first-order approximation (gradient) of loss functions as follows:

$$A^{(t+\frac{1}{2})} = A^{(t)} - \eta^{(t)} \sum_n \partial_{A^{(t)}} \ell(y_n, g(x_n)), \quad (8)$$

where $\eta^{(t)}$ is a step size and $\partial_{A^{(t)}} \ell(\cdot, \cdot)$ is the gradient of loss functions evaluated at $A^{(t)}$. In the proximal step, we apply regularization to the current solution $A^{(t+\frac{1}{2})}$ as follows:

$$A^{(t+1)} = M_0(A^{(t+\frac{1}{2})}) \text{ where } M_0(B) = \operatorname{argmin}_A \left(\frac{1}{2} \|A - B\|_F^2 + \eta^{(t)} \Omega(A) \right), \quad (9)$$

where $\|\cdot\|_F$ is the Frobenius norm. Furthermore, we have adopted a backtracking rule [6] to avoid the difficulty of calculating appropriate step widths beforehand.

We also employ FISTA [6] to achieve a faster convergence rate, $O(1/t^2)$, for weakly convex problems. In FISTA, the proximal operator step (9) is modified with an additional step width $s^{(t)}$ and a matrix $V^{(t)}$ as follows:

$$\begin{aligned} V^{(t)} &= \operatorname{argmin}_V \frac{1}{2} \|V - A^{(t+\frac{1}{2})}\|_F^2 + \eta_t \Omega(V), \\ s^{(t+1)} &= \frac{1 + \sqrt{1 + 4(s^{(t)})^2}}{2}, \\ a_{dp}^{(t+1)} &= v_{dp}^{(t)} + \frac{s^{(t)} - 1}{s^{(t+1)}} (v_{dp}^{(t)} - v_{dp}^{(t-1)}). \end{aligned} \quad (10)$$

where we take $V^{(0)} = A^{(1)}$ and $t^{(1)} = 1$. $V^{(t)}$ is the same as the solution for the original proximal map. In both theoretical analysis and empirical evaluations, we have confirmed that (10) significantly improves convergence in learning partition-wise linear models.

3.2.3 Decomposition of Proximal Maps

The computational cost of the proximal method depends strongly on the efficiency of solving the proximal step (9). A number of approaches have been developed for improving efficiency, including the minimum-norm-point approach [14] and the workflow approach [16, 17]. Their computational efficiencies depend strongly on feature and partition size², however, which makes them inappropriate for our formulation because of potentially large feature and partition sizes.

Alternatively, this paper employs the decomposition of proximal maps [7]. The key idea here is to decompose the proximal step into a sequence of sub-problems that are easily solvable. We first introduce two easily-solvable proximal maps as follows:

$$M_1(B) = \underset{A}{\operatorname{argmin}} \frac{1}{2} \|A - B\|_F^2 + \eta^{(t)} \lambda_P \sum_{p=1}^P \|a_p\|_\infty, \quad (11)$$

$$\begin{aligned} M_2(B) &= \underset{A}{\operatorname{argmin}} \frac{1}{2} \|A - B\|_F^2 + \eta^{(t)} \lambda_0 \sum_{p=0}^P \sum_{d=1}^D \|a_{dp}\|_\infty \\ &= \underset{A}{\operatorname{argmin}} \frac{1}{2} \|A - B\|_F^2 + \eta^{(t)} \lambda_0 \sum_{p=0}^P \sum_{d=1}^D |a_{dp}|. \end{aligned} \quad (12)$$

The theorem below guarantees that the decomposition of the proximal map (9) can be performed.

Theorem 1 *The original problem (9) can be decomposed by using the following two proximal maps as follows:*

$$A^{(t+1)} = M_0(A^{(t+\frac{1}{2})}) = M_2(M_1(A^{(t+\frac{1}{2})})). \quad (13)$$

Proof: From the discussion of Theorem 1 in [7], we can determine the sufficient condition for satisfying this decomposition of proximal maps. The sufficient condition here is:

$$\forall B, p \quad \partial \|a_p\|_\infty \supseteq \partial \|b_p\|_\infty \quad \text{where } A = M_2(B), \quad (14)$$

where $\partial \|a_p\|_\infty$ is a subdifferential set of $\|a_p\|_\infty$. Keys of this proof are 1) properties in the subdifferential of L_∞ norm, and 2) no variance in the magnitude relationship among features as seen before and after soft-thresholding.

The subdifferential of $\|a_p\|_\infty$ is a convex hull of unit vectors with respect to a set of features that indicate the max absolute value in a_p . A set of features having the max absolute value is denoted by Q in this proof. Therefore, formula (14) is satisfied when Q derived from a_p includes all features in Q derived from b_p . $M_2(\cdot)$ is a well-known soft-thresholding operator. This problem can be decomposed into element-wise problems, and the update formula can be described as follows:

$$a_p = \operatorname{sgn}(b_{dp}) \max \left(0, |b_{dp} - \eta^{(t)} \lambda_0| \right). \quad (15)$$

$\eta^{(t)} \lambda_0$ is a constant and is applied to all features. Therefore, Q derived from a_p is the same as Q derived from b_p when $\|b_p\|_\infty > \eta^{(t)} \lambda_0$. When $\|b_p\|_\infty \leq \eta^{(t)} \lambda_0$, all weights become 0 and Q derived from a_p includes all features. As a result, Q derived from a_p always includes all features in Q derived from b_p and the sufficient condition (14) is always satisfied. \square

The first proximal map (11) is the proximal operator with respect to the $L_{1,\infty}$ -regularization. This problem can be decomposed into group-wise sub-problems. Each proximal operator with respect

²For example, the fastest algorithm for the workflow approach has $O(\mathcal{M}(B+1) \log(\mathcal{M}^2/(B+1)))$ time complexity, where B is the number of breakpoints determined by the structure of the graph ($B \leq D(P+1) = O(DP)$) and \mathcal{M} is the number of nodes, that is $P + D(P+1) = O(DP)$ [16]. Therefore, the worst computational complexity is $O(D^2 P^2 \log DP)$.

Algorithm 1 Iterative update procedure in the global and local residual model

Require: Training data $\{(x_n, y_n)\}$, initial step width $\eta^{(1)}$, regularization hyperparameters λ_0, λ_P
Initialize $A^{(1)} \in \mathbb{R}^{D \times (P+1)}$
if Apply **warm start** of the global model **then**
 solve (17) and used its solution as $a_0^{(1)}$
end if
for $t = 1, \dots, T$ **do**
 /* **Gradient Step** */
 Calculate gradient $\partial_{A^{(t)}} \ell(y_n, g(x_n))$ for all n
 Derive $A^{(t+1/2)}$ by calculating (8)
 /* **Proximal Step** */
 Derive $A^{(t+3/4)} = M_1(A^{(t+1/2)})$ by calculating (16)
 Derive $A^{(t+1)} = M_2(A^{(t+3/4)})$ by calculating (15)
 if Apply **acceleration** method **then**
 Update $A^{(t+1)}$ by following (10)
 end if
 /* **Backtracking** */
 if **backtracking rule** is violated **then**
 Halve the value of step width $\eta^{(t+1)} = \eta^{(t)} / 2$
 Restore previous weight matrix $A^{(t+1)} = A^{(t)}$
 else
 Maintain the same step width $\eta^{(t+1)} = \eta^{(t)}$
 end if
 /* **Termination** */
 if the gap of objective values between the current iteration and the previous iteration is less than 10^{-9} in 10 consecutive iterations **then**
 terminate algorithm
 end if
end for

to each group can be computed through a projection on an L_1 -norm ball (derived from the Moreau decomposition [14]), that is,

$$a_p = b_p - \underset{c}{\operatorname{argmin}} \|c - b_p\|_2 \quad \text{s.t.} \quad \|c\|_1 \leq \eta^{(t)} \lambda. \quad (16)$$

This projection problem can be efficiently solved [18].

The second proximal map (12) is a well-known proximal operator with respect to L_1 -regularization. The solution to element-wise problems is described in (15). These two sub-problems can be easily solved, and we can easily obtain the solution for the original proximal map (9).

3.2.4 Time Complexity and Convergence Analysis

Although the time complexity of a single gradient step (8) is $O(NPD)$ with naive full gradient calculation, we can reduce the order by utilizing partition sparseness. In the t -th gradient step, we only need to calculate gradients of active partitions, which in practice are far fewer than with P . A two-stage gradient calculation, i.e., first searching for active partitions and then calculating their gradients, makes the time complexity $O(NP + \hat{P}D)$, where \hat{P} is the number of active partitions.

The time complexity in the proximal steps is dominated by the cost of the calculation of (11) and (12). The first is a simple soft-thresholding operation, and the computational complexity is $O(PD)$. The second is an L_∞ -regularization proximal operation, and the dominant factor is the sorting of features in each group. The computational complexity of feature ordering is $O(D \log D)$, and the time complexity becomes $O(PD \log D)$.

The resulting computational complexity of partition-wise linear models is, then, $O(NP + \hat{P}D + PD \log D)$.

3.2.5 Warm Start of Global Model

Although partition-wise linear models can derive global optimums by means of the proximal method from any initial point, the choice of the initial point considerably affects practical convergence speed. We initialize the global weight vector, using the L_1 -regularization solution, as:

$$a_0^{(1)} = \operatorname{argmin}_{a_0} \sum_n \ell(y_n, a_0^T x_n) + \lambda_0 \|a_0\|_1. \quad (17)$$

The local weight vectors are uniformly initialized. Empirical comparisons among such few initialization methods as random initialization, zero initialization, etc. indicate that this initialization reliably achieves better empirical convergence. The result is denoted in Section 5.2.3.

The iterative update procedure for the global and local residual is expressed, then, in Algorithm 1.

4 Generalization Bound Analysis

This section presents the derivation of a generalization error bound for partition-wise linear models and discusses how we can increase the number of partition candidates P over the number of samples N . Our bound analysis is related to that of [19], which gives bounds for general overlapping group Lasso cases, while ours is specifically designed for partition-wise linear models.

Let us first derive an empirical Rademacher complexity [20] for a feasible weight space conditioned on (7). The definition of Rademacher complexity is as follows:

$$\mathfrak{R}_X(A) = \frac{2}{n} \mathbb{E} \left[\sup_{A \in \mathcal{A}} \sum_{n=1}^N \epsilon_i g(x_i) \right]. \quad (18)$$

where $X = (x_1, x_2, \dots, x_N)$. The expectation is over all ϵ_i , which are i.i.d. $\{\pm 1\}$ -valued random variables. We can derive Rademacher complexity for our model using the Lemma below. This Lemma is used to derive the upper bound of the expected loss.

Lemma 1 *If $\Omega(A) \leq 1$ is satisfied and if almost surely $\|x\|_\infty \leq 1$ with respect to $x \in \mathcal{X}$, the empirical Rademacher complexity for partition-wise linear models can be bounded as:*

$$\frac{2^{3/2}}{\sqrt{N}} \left(2 + \sqrt{\ln(P + D(P + 1))} \right). \quad (19)$$

Proof: Let us vectorize a weight matrix A into $\mathbf{a} = (a_1^T, a_2^T, \dots, a_P^T)^T$. By using this notation, (7) is reformulated as:

$$\Omega(A) = \lambda_P \sum_{p=1}^P \|u_p \otimes \mathbf{a}\|_\infty + \lambda_0 \sum_{p=0}^P \sum_{d=1}^D \|u_{dp} \otimes \mathbf{a}\|_\infty, \quad (20)$$

where \otimes is a Kronecker product, u_{dp} is a basis vector w.r.t. the d -th feature of the p -th partition, and $u_p = \sum_d u_{dp}$. This is a special case of Theorem 2 of [19] in which the number of groups is $P + D(P + 1)$. The assumptions here are $\Omega(A) \leq 1$, $\|f_p(x)x\|_\infty \leq 1$ for all $p \geq 1$, and $|f_p(x)x_d| \leq 1$ for all d, p almost surely with respect to $x \in \mathcal{X}$. The second and third assumptions are satisfied when $\|x\|_\infty \leq 1$ is satisfied. It can be proved from the definition of the L_∞ norm that

$$1 \geq \|x\|_\infty = \|f_0(x)x\|_\infty \geq \|f_p(x)x\|_\infty = \max_d |f_p(x)x_d| \geq |f_p(x)x_d|. \quad (21)$$

Applying Theorem 2 of [19] to (20) gives us (19). \square

The next theorem shows the generalization bound of the global and local residual model. This bound is straightforwardly derived from Lemma 1 and the discussion of [20]. In [20], it has been shown that the uniform bound on the estimation error can be obtained through the upper bound of Rademacher complexity derived in Lemma 1. By using the uniform bound, the generalization bound of the global and local residual model defined in formula (4) can be derived.

Theorem 2 Let us define a set of weights that satisfies $\Omega_{group}(A) \leq 1$ as \mathcal{A} where $\Omega_{group}(A)$ is as defined in Section 2.5 in [19]. Let a datum (x_n, y_n) be i.i.d. sampled from a specific data distribution \mathcal{D} and let us assume loss functions $\ell(\cdot, \cdot)$ to be L -Lipschitz functions with respect to a norm $\|\cdot\|$ and its range to be within $[0, 1]$. Then, for any constant $\delta \in (0, 1)$ and any $A \in \mathcal{A}$, the following inequality holds with probability at least $1 - \delta$.

$$\mathbb{E}_{(x,y) \sim \mathcal{D}} [\ell(y, g(x))] \leq \frac{1}{N} \sum_{n=1}^N \ell(y_n, g(x_n)) + \frac{2^{3/2}L}{\sqrt{N}} \left(2 + \sqrt{\ln(DP + P + D)} \right) + \sqrt{\frac{\ln 1/\delta}{2N}}. \quad (22)$$

This theorem implies how we can increase the number of partition candidates. The third term of the right-hand side is obviously small if N is large. The second term converges to zero with $N \rightarrow \infty$ if the value of P is smaller than $o(e^N)$, which is a sufficiently large number in practice. In summary, we expect to be able to handle a sufficient number of partition candidates for learning with little risk of over fitting.

5 Experiments

We conducted two types of experiments: 1) evaluation of how partition-wise linear models perform, on the basis of a simple synthetic dataset and 2) comparisons with state-of-the-art region-specific and locally linear models on the basis of standard classification and regression benchmark datasets.

5.1 Evaluation Using Synthetic Dataset

We generated a synthetic binary classification dataset as follows. x_n s were uniformly sampled from a 20-dimensional input space in which each dimension had values between $[-1, 1]$. The target variables were determined using the XOR rule over the first and second features (the other 18 features were added as noise for prediction purposes.), i.e., if the signs of first feature value and second feature value are the same, $y = 1$, otherwise $y = -1$. This is well known as a case in which linear models do not work. For example, L_1 -regularized logistic regression produced nearly random outputs where the error rate was 0.421.

We generated one partition for each feature except for the first feature. Each partition became active if the corresponding feature value was greater than 0.0. Therefore, the number of candidate partitions was 19. We used the logistic regression function for loss functions. Hyper-parameters³ were set as $\lambda_0 = 0.01$ and $\lambda_P = 0.001$. The algorithm was run in 1,000 iterations.

Figure 2 illustrates results produced by the global and local residual model. The left-hand figure illustrates a learned effective partition (red line) to which the weight vector $a_1 = (10.96, 0.0, \dots)$ was assigned. This weight a_1 was only applied to the region above the red line. By combining a_1 and the global weight a_0 , we obtained the piece-wise linear representation shown in the right-hand figure. While it is yet difficult for existing piece-wise linear methods to capture global structures⁴, our convex formulation makes it possible for the global and local residual model to easily capture the global XOR structures.

5.2 Comparisons Using Benchmark Datasets

We next used benchmark datasets to compare our models with other state-of-the-art region-specific models. In these experiments, we simply generated partition candidates (activeness functions) as follows. For continuous value features, we calculated all 5-quantiles for each feature and generated partitions at each quantile point. Partitions became active if a feature value was greater than the corresponding quantile value. For binary categorical features, we generated two partitions in which

³We conducted several experiments on other hyper-parameter settings and confirmed that variations in hyper-parameter settings did not significantly affect results.

⁴For example, a decision tree cannot be used to find a “true” XOR structure since marginal distributions on the first and second features cannot discriminate between positive and negative classes.

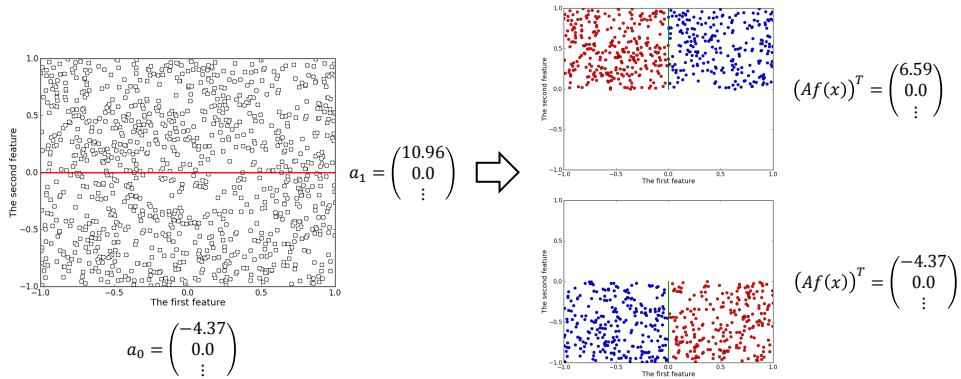


Figure 2: How the global and local residual model classifies XOR data. Red line indicates effective partition; green lines indicate local predictors; red circles indicate samples with $y = -1$; blue circles indicate samples with $y = 1$: This model classified XOR data precisely.

Table 3: Classification and regression datasets. N is the size of data. D is the number of dimensions. P is the number of partitions. CL/RG denotes the type of dataset (CL: Classification/RG: Regression).

	N	D	P	CL/RG
skin	245,057	3	12	CL
winequality	6,497	11	44	CL
census_income	45,222	105	99	CL
twitter	140,707	11	44	CL
a1a	1,605	113	452	CL
breast-cancer	683	10	40	CL
internet_ad	2,359	1,559	1,558	CL
energy_heat	768	8	32	RG
energy_cool	768	8	32	RG
abalone	4,177	10	40	RG
kinematics	8,192	8	32	RG
puma8NH	8,192	8	32	RG
bank8FM	8,192	8	32	RG
communities	1,994	101	404	RG

one became active when the feature was 1 (yes) and the other became active only when the feature value was 0 (no).

We utilized several standard classification and regression benchmark datasets from UCI datasets (skin, winequality, census_income, twitter, internet_ad, energy_heat, energy_cool, communities), libsvm datasets (a1a, breast_cancer), and LIACC datasets (abalone, kinematics, puma8NH, bank8FM). Table 3 summarizes specifications for each dataset.

5.2.1 Classification

For classification, we compared the global and local residual model (Global/Local) with L_1 logistic regression (Linear), LSL-SP with linear discrimination analysis⁵, LDKL supported by L_2 -

⁵The source code is provided by the author of [3].

Table 4: Classification results: error rate (standard deviation). The best performance figure in each dataset is denoted in **bold** typeface and the second best is denoted in *bold italic*.

	Linear	Global/Local	LSL-SP	LDKL	FaLK-SVM	RBF-SVM
skin	8.900 (0.174)	0.249 (0.048)	12.481 (8.729)	1.858 (1.012)	0.040 (0.016)	0.229 (0.029)
winequality	33.667 (1.988)	23.713 (1.202)	30.878 (1.783)	36.795 (3.198)	28.706 (1.298)	23.898 (1.744)
census_income	43.972 (0.404)	35.697 (0.453)	35.405 (1.179)	47.229 (2.053)	–	45.843 (0.772)
twitter	6.964 (0.164)	4.231 (0.090)	8.370 (0.245)	15.557 (11.393)	4.135 (0.149)	9.109 (0.160)
ala	16.563 (2.916)	16.250 (2.219)	20.438 (2.717)	17.063 (1.855)	18.125 (1.398)	16.500 (1.346)
breast-cancer	35.000 (4.402)	3.529 (1.883)	3.677 (2.110)	35.000 (4.402)	–	33.824 (4.313)
internet_ad	7.319 (1.302)	2.638 (1.003)	6.383 (1.118)	13.064 (3.601)	3.362 (0.997)	3.447 (0.772)

regularized hinge loss⁶, FaLK-SVM with linear kernels⁷, and C-SVM with RBF kernel⁸. Note that C-SVM is neither a region-specific nor locally linear classification model; it is, rather, a non-linear model. We compared it with ours as a reference with respect to a common non-linear classification model.

For our models, we used logistic functions for loss functions. The max iteration number was set as 1000, and the algorithm stopped early when the gap in the empirical loss from the previous iteration became lower than 10^{-9} in 10 consecutive iterations. Hyperparameters⁹ were optimized through 10-fold cross validation. We fixed the number of regions to 10 in LSL-SP, tree-depth to 3 in LDKL, and neighborhood size to 100 in FaLK-SVM.

Table 4 summarizes the classification errors. We observed:

- Global/Local consistently performed well and achieved the best error rates for four datasets out of seven.
- LSL-SP performed well for census_income and breast-cancer, but did significantly worse than Linear for skin, twitter, and ala. Similarly, LDKL performed worse than Linear for census_income, twitter, ala and internet_ad. This arose partly because of over fitting and partly because of bad local minima. Particularly noteworthy is that the standard deviations in LDKL were much larger than in the others, and the initialization issue would seem to become significant in practice.
- FaLK-SVM performed well in most cases, but its computational cost was significantly higher than that of others, and it was unable to obtain results for census_income and internet_ad (we stopped the algorithm after 24 hours running).

5.2.2 Regression

For regression, we compared Global/Local with Linear, regression tree¹⁰ by CART (RegTree) [1], and epsilon-SVR with RBF kernel¹¹. Target variables were standardized so that their mean was 0 and their variance was 1. Performance was evaluated using the root mean squared loss in the test data. Tree-depth of RegTree and ϵ in RBF-SVR were determined by means of 10-fold cross validation. Other experimental settings were the same as those used in the classification tasks.

Table 5 summarizes RMSE values. In classification tasks, Global/Local consistently performed well. For the kinematics, RBF-SVR performed much better than Global/Local, but Global/Local was better than Linear and RegTree in many other datasets.

5.2.3 Warm Start Effect

We also conducted time comparisons between our partition-wise linear models with and without warm start. We used the ala dataset for the comparisons and considered the relationship between

⁶<https://research.microsoft.com/en-us/um/people/manik/code/LDKL/download.html>

⁷<http://disi.unitn.it/~segata/FaLKM-lib/>

⁸We used a libsvm package for the experiment. <http://www.csie.ntu.edu.tw/~cjlin/libsvm/>

⁹ λ^1, λ_p^2 in Global/Local, λ^1 in Linear, $\lambda_W, \lambda_\theta, \lambda_{\theta'}, \sigma$ in LDKL, C in FaLK-SVM, and C, γ in RBF-SVM.

¹⁰We used a scikit-learn package. <http://scikit-learn.org/>

¹¹We used a libsvm package.

Table 5: Regression results: root mean squared loss (standard deviation). The best performance figure in each dataset is denoted in **bold** typeface and the second best is denoted in *bold italic*.

	Linear	Global/Local	RegTree	RBF-SVR
energy_heat	0.480 (0.047)	0.101 (0.014)	0.050 (0.005)	0.219 (0.017)
energy_cool	0.501 (0.044)	0.175 (0.018)	0.200 (0.018)	0.221 (0.026)
abalone	0.687 (0.024)	0.659 (0.023)	0.727 (0.028)	0.713 (0.025)
kinematics	0.766 (0.019)	0.634 (0.022)	0.732 (0.031)	0.347 (0.010)
puma8NH	0.793 (0.023)	0.601 (0.017)	0.612 (0.024)	0.571 (0.020)
bank8FM	0.255 (0.012)	0.218 (0.009)	0.254 (0.008)	0.202 (0.007)
communities	0.586 (0.049)	0.578 (0.040)	0.653 (0.060)	0.618 (0.053)

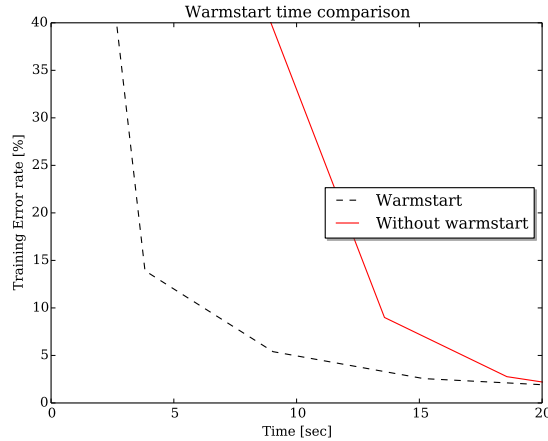


Figure 3: Time comparison between partition-wise linear models with and without warm start

training error rate and computational time. Figure 3 shows the results. It indicates that our models with warm start achieved lower training error rates than did models without warm start.

6 Discussion

6.1 Scaling Up Optimization

In dealing with large-scale data in which the number of samples is very large, full gradient calculation (8) becomes a computational bottleneck. For scaling up our algorithm, stochastic and parallel optimization techniques appear promising. With respect to stochastic optimization, Mairal has recently proposed Minimization by Incremental Surrogate Optimization (MISO) [21] as an incremental optimization method for a majorization-minimization framework that includes proximal methods. Despite the fact that MISO stochastically approximates gradients (sampling), it has a linear convergence property for the global optimum when the data size is known in advance; this convergence rate is the same as the one in the full gradient case. Another promising direction is parallelization. Parallelization of full gradient calculations is a straightforward process and could be of insignificant importance in actual practice. Another possible future direction is a greedy solver for original non-convex problems (4), such as orthogonal matching pursuits [22].

6.2 Advanced Partition Generation

In Section 5, we generated partition candidates (activeness functions) on the basis of simple rules. Although this worked reasonably, more advanced partition generation methods might improve predictive accuracy. Taking locally linear SVMs [10] as an analogy, it is known that local coordinate (anchor) selection considerably affects predictive performance, and advanced coordinate generation

methods have been proposed [11, 12]. The algorithm proposed by Dekel and Shamir [23] gradually adds piece-wise regions on the basis of the detection of “poorly predictable” regions, and it trains piece-wise predictors. While this approach is not directly-applicable to partition-wise linear models, such a “boosting-type” approach to partition candidate generation is an interesting concept to consider.

6.3 Hierarchical Structured Sparseness

In this study, we have treated partition candidates equally and enforced the group sparse penalty. In many real applications, data have structures, and it would be interesting to incorporate such structures into the learning process in partition-wise linear models. In this regard, the “tree-structured” sparsity-inducing regularization proposed by Huang et al. [24] is particularly notable. Defining hierarchical partition structures and automatically learning “hierarchical” region structures might give us an improved understanding of data structures. Note that such tree-structured regularization is also convex, and we might directly apply it to our optimization technique.

7 Summary

We have proposed here a novel convex formulation of region-specific linear models that we refer to as partition-wise linear models. Our approach simultaneously optimizes regions and predictors using sparsity-inducing structured penalties. For the purpose of efficiently solving the optimization problem, we have derived an efficient algorithm based on the decomposition of proximal maps. Thanks to its convexity, our method is free from initialization dependency, and a generalization error bound can be derived. Empirical results demonstrate the superiority of partition-wise linear models over other region-specific and locally linear models.

Acknowledgments

The majority of the work was done during the internship of the first author at the NEC central research laboratories.

References

- [1] Leo Breiman, J. H. Friedman, R. A. Olshen, and C. J. Stone. *Classification and Regression Trees*. Wadsworth, 1984.
- [2] Cijo Jose, Prasoon Goyal, Parv Aggrwal, and Manik Varma. Local deep kernel learning for efficient non-linear svm prediction. In *ICML*, pages 486–494, 2013.
- [3] Joseph Wang and Venkatesh Saligrama. Local supervised learning through space partitioning. In *NIPS*, pages 91–99, 2012.
- [4] Zhixiang Xu, Matt Kusner, Minmin Chen, and Kilian Q. Weinberger. Cost-Sensitive Tree of Classifiers. In *ICML*, pages 133–141, 2013.
- [5] Paul Tseng. Approximation accuracy, gradient methods, and error bound for structured convex optimization. *Mathematical Programming*, 125(2):263–295, 2010.
- [6] Amir Beck and Marc Teboulle. A fast iterative shrinkage-thresholding algorithm for linear inverse problems. *SIAM Journal on Imaging Sciences*, 2(1):183–202, 2009.
- [7] Yaoliang Yu. On decomposing the proximal map. In *NIPS*, pages 91–99, 2013.
- [8] Michael I. Jordan and Robert A. Jacobs. Hierarchical mixtures of experts and the em algorithm. *Neural Computation*, 6(2):181–214, 1994.
- [9] Nicola Segata and Enrico Blanzieri. Fast and scalable local kernel machines. *Journal of Machine Learning Research*, 11:1883–1926, 2010.
- [10] Lubor Ladicky and Philip H.S. Torr. Locally Linear Support Vector Machines. In *ICML*, pages 985–992, 2011.
- [11] Kai Yu, Tong Zhang, and Yihong Gong. Nonlinear learning using local coordinate coding. In *NIPS*, pages 2223–2231, 2009.

- [12] Ziming Zhang, Lubor Ladicky, Philip H.S. Torr, and Amir Saffari. Learning anchor planes for classification. In *NIPS*, pages 1611–1619, 2011.
- [13] Quanquan Gu and Jiawei Han. Clustered support vector machines. In *AISTATS*, pages 307–315, 2013.
- [14] Francis R. Bach. Structured sparsity-inducing norms through submodular functions. In *NIPS*, pages 118–126, 2010.
- [15] Yurii Nesterov. Gradient methods for minimizing composite objective function. Core discussion papers, 2007.
- [16] Giorgio Gallo, Michael D. Grigoriadis, and Robert E. Tarjan. A fast parametric maximum flow algorithm and applications. *SIAM Journal on Computing*, 18(1):30–55, 1989.
- [17] Kiyohito Nagano and Yoshinobu Kawahara. Structured convex optimization under submodular constraints. In *UAI*, 2013.
- [18] John Duchi and Yoram Singer. Efficient online and batch learning using forward backward splitting. *Journal of Machine Learning Research*, 10:2899–2934, 2009.
- [19] Andreas Maurer and Massimiliano Pontil. Structured sparsity and generalization. *Journal of Machine Learning Research*, 13:671–690, 2012.
- [20] Peter L. Bartlett and Shahar Mendelson. Rademacher and gaussian complexities: risk bounds and structural results. *Journal of Machine Learning Research*, 3:463–482, 2002.
- [21] Julien Mairal. Optimization with first-order surrogate functions. In *ICML*, pages 783–791, 2013.
- [22] Y.C. Pati, R. Rezaifar, and P.S. Krishnaprasad. Orthogonal matching pursuit: Recursive function approximation with applications to wavelet decomposition. In *ASLOMAR*, pages 40–44, 1993.
- [23] Ofer Dekel and Ohad Shamir. There’s a hole in my data space: Piecewise predictors for heterogeneous learning problems. In *AISTATS*, pages 291–298, 2012.
- [24] Junzhou Huang, Tong Zhang, and Dimitris N. Metaxas. Learning with structured sparsity. *Journal of Machine Learning Research*, 12:3371–3412, 2011.